Pharmaceutical Sciences Asia

Pharm Sci Asia 2024; 51(2), 106-117

DOI:10.29090/psa.2024.02.24.906

Research Article

Nanosponge as a novel delivery modulator of retinoic acid

Sharifah Shakirah Syed Omar[1,3], Hazrina Ab Hadi[1,2*], Abd Almonem Doolanea[1,4], Nuraqilah Zulkifli[1,2]

[1] Dermatopharmaceutics Research Group, International Islamic University Malaysia, Kuantan, Pahang, Malaysia
[2] Department of Pharmaceutical Technology, Faculty of Pharmacy, International Islamic University Malaysia, Kuantan, Pahang, Malaysia
[3] Department of Pharmaceutical Technology, Faculty of Pharmacy, University Malaya, Kuala Lumpur, Malaysia
[4] Sabrena Experience, 1500 Dragon Street, Suite 160, Dallas, Texas

ABSTRACT

Retinoic acid is a derivative of vitamin A known for its use in the management of acne. The major limitations of retinoic acid application are its low solubility and instability in water, light, and heat. It also causes irritating side effects on the skin when used topically. In the current work, we demonstrated the entrapment of retinoic acid into nanosponge to improve the solubility and delivery of retinoic acid for skin application. The entrapment of retinoic acid into nanosponge was investigated by varying polymer: crosslinker ratio, duration of homogenization, and drug: nanosponge ratio. High entrapment efficiency was achieved with nanosponge at 73.90%. The entrapment was confirmed through several characterizations including Attenuated Total Reflection Fourier Transform Infrared (ATR-FTIR), Differential Scanning Calorimetry (DSC), and Field Emission Scanning Electron Microscopy (FESEM). Higher solubilization was achieved with retinoic acid-loaded nanosponge compared to free drug. Franz cell studies show that the entrapment of retinoic acid in nanosponge slowed the release of retinoic acid and allowed it to remain within the skin layers longer.

Keywords:
Retinoic Acid, Tretinoin, Nanosponge, Cyclodextrin

1. INTRODUCTION

Tretinoin or retinoic acid was found to be one of the retinoids with the highest efficacy against acne compared to more recent retinoids such as adapalene[1-2]. Retinoids act by normalizing desquamation by promoting differentiation and reducing keratinocyte proliferation. The anti-inflammatory actions take place by blocking inflammatory pathways involving toll-like receptors, leukocyte migration, and the AP-1 pathway which inhibits inflammation by reducing the release of cytokines and nitric oxide. Other than targeting acne, retinoids can also improve secondary acne lesions, in particular acne scarring and pigmentation. Scarring is improved by upregulation of procollagen genes while pigmentation is reduced by accelerating epidermal turnover and inhibition of melanosome transfer[3]. However, it has a greater skin irritation risk compared to other retinoids. The use of retinoids is limited by its side effects such as peeling, dryness, erythema, desquamation, burning, and pruritus, especially in those with sensitive skin[3-4]. Chemical-wise, retinoic acid is insoluble in water, and unstable in the presence of air, light, and heat[5]. These challenges make retinoic acid unstable due to its photosensitivity and proneness to oxidative degradation in aqueous solution. Hence it is necessary to overcome these challenges to maximize the benefits of retinoic acid effectively.

In this study, the objective is to prepare a nanosponge loaded with retinoic acid for the topical treatment of acne. Nanosponge is a novel drug delivery system developed to improve the delivery of existing drugs. Studies have been done researching the use of nanosponge in delivering a diverse range of drugs with various delivery routes gaining positive results[6-9]. Delivering drugs using nanosponge has been garnering attention because it helps reduce dose, and provide controlled and sustained release along with enhancement of stability[10-11]. These advantages in the formulation development phase will benefit the end-users of drugs in the long run. Cyclodextrin-based nanosponges are one of the classes of nanosponges that has been used

***Corresponding author:**
*Hazrina Ab Hadi Email: hazrina@iium.edu.my

extensively in current research attributed to their nanocavities that can entrap lipophilic and hydrophilic chemical substances[12].

Cyclodextrins are part of cyclic glucopyranose oligomers that have a cage-like structure with a lipophilic cavity. The interaction of cyclodextrin with a cross-linker improves the formation of a solid material with high porosity and intertwined microchannels[13]. β-cyclodextrin is largely opted for in the development of nanosponges because of its nano-sized cavities, cost-effectiveness, easy availability, and most importantly high complexing ability with cross-linking agents[10,12]. β-cyclodextrin based nanosponge can be classified into carbamate, carbonate, ester, poly amidoamine, or modified and cyclodextrin-calixarene nanosponge which differ based on the methods of preparation, solvents, and crosslinkers used[12]. Nanosponge proves to be versatile and can be adjusted to suit the type of drug that requires improvement in its delivery. The use of nanosponge in topical delivery is also very promising due to its slow release which can reduce skin irritation while maintaining constant efficacy[7,14-15].

2. MATERIALS AND METHODS

The solvent used Dimethylformamide (DMF) and methanol was obtained from Fisher Scientific (Massachusetts, USA). Nanosponge preparation used anhydrous β-cyclodextrin (BCD) as the polymer and carbonyldiimidazole (CDI) as the crosslinker which was obtained from Acros Organics (Geel, Belgium). Phosphate buffer saline (PBS) was procured from Sigma Life Science, Sigma Aldrich Co. (St Louis, USA).

2.1. Nanopsonge preparation

A jacketed beaker connected to a water bath maintained at 90°C was set up for the nanosponge development. DMF which acts as a solvent was added to the beaker and maintained at 90°C. BCD was dried overnight in an oven at 50°C. When DMF reached 90°C, BCD was dissolved forming a clear solution then CDI was also added. The reaction was performed for 3 hours producing a solid block. The solid produced was washed with water followed by acetone through a vacuum filtration system. The solid collected was purified through Soxhlet extraction with absolute ethanol for 24 hours and then crushed. The ratio of polymer to crosslinker (polymer: crosslinker) was varied at 1:2, 1:4, and 1:8 as shown in Table 1.

2.2. Particle size reduction of nanosponge

The nanosponge was then subjected to homogenization using WiseTis HG-15D digital homogenizer (Witeg Labortechnik, Wertheim, Germany) to reduce the particle size. 5 g of nanosponge was suspended in distilled water and homogenized at 2,000 rpm with varying durations of 10 minutes, 15 minutes, and 20 minutes. The nanosponge was then centrifuged at 5,000 rpm for 15 minutes and freeze-dried for 24 hours. The factors investigated to optimize the nanosponge were the ratio of polymer: crosslinker and duration of homogenization as shown in Table 2. The particle size, polydispersity index, and zeta potential were the dependent variables studied and optimized with factorial design. The best nanosponge was selected and used for the entrapment of retinoic acid.

2.3. Retinoic acid entrapment in nanosponge

A 10 mg/ml aqueous suspension of nanosponge was prepared with distilled water. Retinoic acid was dispersed into the aqueous suspension at different ratios of 1:2, 1:4, and 1:6 (drug: nanosponge w/w). The suspension was sonicated for 15 minutes and then stirred for 24 hours at ambient temperature in a dark room. After 24 hours the sample was centrifuged at 3,000 rpm for 10 minutes and the supernatant was collected. The supernatant was then freeze-dried using Alpha 1-2 LDplus Freeze Dryer (Martin Christ®, Osterode am Harz, Germany) for 24 hours[16-17].

Table 1. Variation of BCD and CDI at each ratio.

Polymer:crosslinker	Amount of BCD		Amount of CDI	
1:2	4.4 mmol	5g	8.8 mmol	1.43 g
1:4	4.4 mmol	5g	17.6 mmol	2.86 g
1:8	4.4 mmol	5g	35.2 mmol	5.71 g

Table 2. Different nanosponge formulation prepared with varying factors.

Polymer:crosslinker	Duration of homogenization	Nanosponge preparation
1:2	10 minutes	NS1
	15 minutes	NS2
	20 minutes	NS3
1:4	10 minutes	NS4
	15 minutes	NS5
	20 minutes	NS6
1:8	10 minutes	NS7
	15 minutes	NS8
	20 minutes	NS9

2.4. Quantitative determination of retinoic acid by High-Performance Liquid Chromatography (HPLC)

The HPLC analysis of retinoic acid was done using an isocratic system with HPLC 1200 Series (Agilent Technologies, California) The column used was a C-18 silica-based column (ZORBAX, Eclipse Plus, Agilent Technologies) which makes it a reverse phase chromatography. Methanol and 0.5% acetic acid in water with a ratio of 90:10 was used as the mobile phase. The isocratic elution was performed at room temperature with a flow rate and injection volume of 1.0 ml/min and 20 µL respectively. Standard stock solution strength was prepared at 0.2 mg/mL while the standard solutions were prepared ranging from 5-90 µg/mL. All prepared samples were filtered through a 0.45 µm syringe filter. Samples were injected in triplicates and the chromatogram was detected at wavelength 350 nm. The calibration curve was recorded, and a linear regression was observed with a correlation coefficient of 0.997.

2.5. Determination of entrapment efficiency

1 mg of loaded nanosponge was dispersed in 1 ml of methanol and then sonicated for 15 minutes at room temperature. The amount of retinoic acid loaded in the nanosponge was determined through a quantitative estimate of retinoic acid by HPLC analysis in triplicates after filtration of the sonicated sample[9,17-18]. The percentage of retinoic acid loaded into the nanosponge was calculated.

2.6. Determination of solubilization efficiency

The solubility of retinoic acid was assessed using the shake flask method. Retinoic acid was added in excess (12.5 mg) to 5 mL distilled water in a flask and another flask containing a fixed amount of nanosponge (5 mg). Both flasks were sealed and shaken for 24 hours at room temperature in the dark using a mechanical shaker at 100 rpm. The sample was then centrifuged at 6,000 rpm for 20 minutes and the supernatant was collected. Methanol was added to the supernatant and sonicated for 15 minutes before filtration for analysis. The filtrate was analyzed in triplicates with HPLC to determine the concentration of dissolved retinoic acid[9,16-17].

2.7. Particle size and zeta potential analysis

Particle size and zeta potential of the nanosponge were determined using Zetasizer (ZEN 1600, Malvern, UK). Nanosponges were diluted 10 times using distilled water as a dispersant before being analyzed in triplicate[18-19].

2.8. Determination of surface morphology

The shape and surface topography of nanosponge and nanosponge loaded with retinoic acid were evaluated through the FESEM model JSM-7800F Prime (JEOL, Tokyo, Japan) using an acceleration voltage of 5-7kV. Samples were coated with a thin gold-palladium layer before being placed on a glass slide and kept under vacuum. Nanosponge was recorded under magnification ranging from 3,000x to 30,000x[20-21].

2.9. ATR-FTIR spectroscopy study

Analysis was done using Spectrum RX Two Instrument (PerkinElmer Inc., USA) complete with Spectrum 3.5 software. Each sample was placed on the zinc selenide crystal and was run a total of 16 scans at a scanning range of 400 cm^{-1} - 4,000 cm^{-1} with a temperature of 25°C.

2.10. DSC study

Thermal analysis was carried out with a DSC from Netzsch model DSC214 Polyma with the Netzsch Proteous® software (Selb, Germany). Samples of the retinoic acid, blank nanosponge, and retinoic acid loaded nanosponge were analyzed using standard alumina with aluminium sample pans whereby an empty pan was used as the reference standard. 5 mg samples in aluminum pans were heated at a range from 30°C to 300°C under a nitrogen atmosphere with a heating rate of 10°C per minute[17].

2.11. *In vitro* Franz diffusion cells study

An *in vitro* drug release study was done using 8 sets of vertical Franz cells. A finite study was done using dorsal skin from Sprague Dawley rat as the membrane. The skin was obtained ethically with an ethical approval number (IACUC-2020-025) obtained from the Institutional Animal Care and Use Committee (I-ACUC). A study was done with similar strength (0.05%), commercial retinoic acid cream formulation (stearyl alcohol, isopropyl myristate, polyoxyl 40 stearate, xanthan gum, acid sorbic, stearic acid, butylated hydroxytoluene, water) and a retinoic acid loaded nanosponge gel-cream formulation (water, hydroxy ethyl cellulose, lecithin, glycerin, squalane, propylene glycol, tocopherol acetate, phenoxyethanol, ethyl hexylglycerin). The receptor chamber was filled with phosphate buffer saline and methanol solution at a 2:1 v/v ratio and placed on a stirring plate submerged in a water bath at 37°C to maintain the skin at 32°C. 10 mg/cm^2 of the formulation was applied onto the skin and distributed homogenously. Samples were taken at 0.5 1, 2 3, 4, 5, 6, 8, 12, and 24 hours, and the same amount of medium was replenished each time to maintain sink conditions. The cumulative drug amount was calculated and plotted. After washing the skin surface, the skin left was cut into small pieces and soaked in methanol for 24 hours with continuous shaking at 150 rpm for 24 hours

Table 3. Main effect and interaction plot for parameters varied in nanosponge development.

Main Effects Plot	Interaction Plot
Particle size	
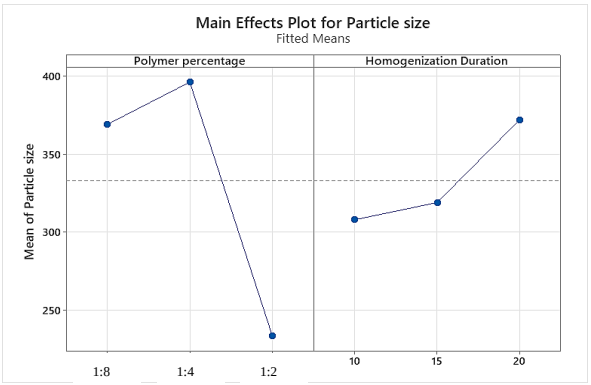	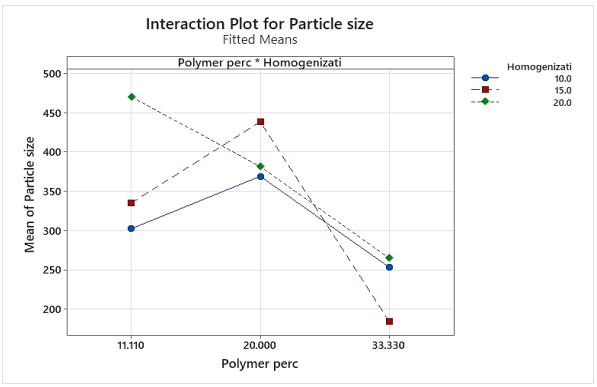
Polydispersity Index	
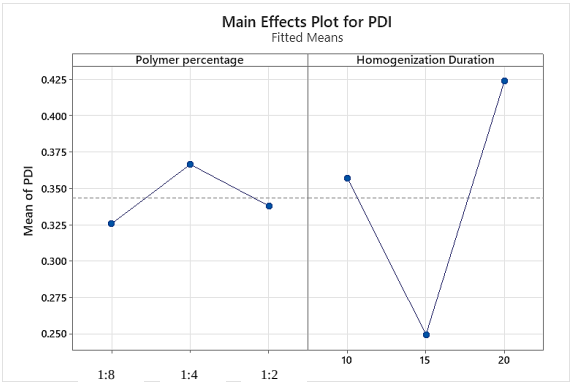	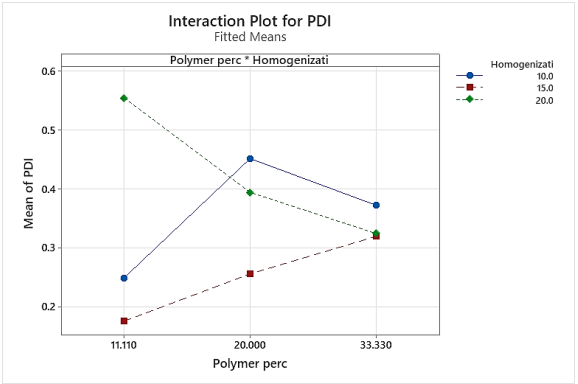
Zeta Potential	
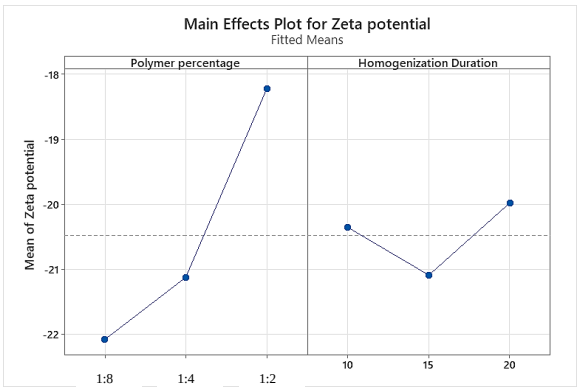	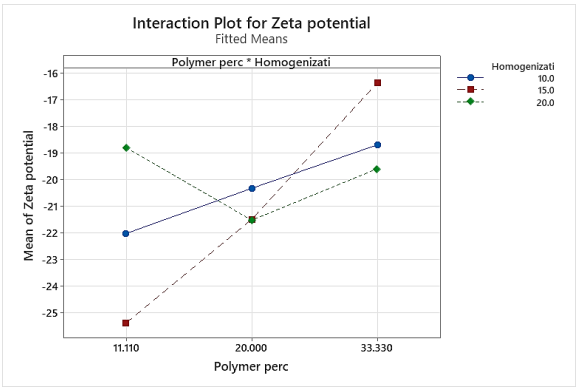

to extract remaining retinoic acid. All samples were analysed with HPLC. The recovery was calculated from the equation below where T is total recovery, P is permeation, W is washings and E is extraction.

$$T=P+W+E$$

3. RESULTS AND DISCUSSION

3.1. Nanosponge development and optimization

3.1.1. Factorial design analysis of nanosponge development

The measured particle size, polydispersity index (PDI), and zeta potential for the varying polymer to crosslinker ratio and homogenization time were analysed with 3^2 factorial design in design of experiment using Minitab software. The independent variable or the cause in this analysis is the polymer: crosslinker ratio and homogenization time. Particle size, PDI, and zeta potential are the

dependent variables or effects. The main effects plot and interaction plot are presented in Table 3. The main effect plot is the effect of an independent variable on the dependent variable while the interaction plot is the effect of independent variables interacting on the dependent variable.

3.1.2. Particle size

Particle size is significantly affected by polymer: crosslinker ratio (p=0.000) and homogenization duration (p=0.003). The interaction of these factors also has a significant effect on particle size (p=0.003). The main effect plot shows the smallest particle size a 1:2 and at 10 minutes respectively. However, the homogenization duration does show an increasing trend in particle size with a longer duration of homogenization. An increase in homogenization time caused an increase in the applied total energy of the system which in turn increases particle coalition and leads to the formation of larger particles. A previous study found that with a mixing time of more than 15 minutes, the increase in particle sizes was greater (p<0.05)[22]. The interaction plot depicts that the smallest particle size was obtained at a ratio of 1:2 with a homogenization duration of 15 minutes while the largest size was at 1:8 with a homogenization duration of 20 minutes. Generally, ratio 1:2 produced the smallest particle size due to the lower crosslinking density which is related to the polymer: crosslinker ratio. The crosslinking density affects the chemical composition and physical properties which include particle size. At a ratio of 1:2, the nanosponge has the lowest amount of crosslinker which means it has lower crosslinking density producing particles that are less hard and easier to be subjected to size reduction[23].

3.1.3. Polydispersity index

Polymer: crosslinker ratio was not significant to PDI and can be seen from the main effect plot which shows that the PDI values fluctuate slightly from one another. On the other hand, homogenization duration does show greater fluctuations which is reflected in the data analysis that found the significant effect of homogenization duration on PDI (p<0.005). The interaction of the two factors was also found to have a significant effect on PDI (p= 0.000). From the interaction plot, the lowest PDI is obtained at a ratio of 1:8 with 15 minutes homogenization duration, and the highest PDI at a ratio of 1:8 with 20 minutes homogenization duration. Based on these results, 15 minutes is the optimum duration for a small PDI as the PDI is low for all ratios. A larger PDI, specifically at 20 minutes homogenization duration seems to correspond with the large particle size most likely produced through particle coalition. Coalition in a vessel can occur between particle and particle, vessel or repeller, and lead to particle agglomeration hence the large size and distribution[24-25].

3.1.4. Zeta potential

Both factors and their interaction significantly affected zeta potential (p=0.000). At a higher polymer: crosslinker ratio, zeta potential increases. From the main effects plot, a higher polymer to crosslinker ratio (1:8) causes lower zeta potential, while homogenization duration shows the lowest zeta potential at 15 minutes. The interaction plot shows that at 10 and 15 minutes there is an increasing trend of the zeta potential as the polymer: crosslinker ratio decreases. Particle size is one of the factors affecting zeta potential whereby the smaller the particle size the greater the value of the zeta potential[26].

3.2. Characterization of retinoic acid-loaded nanosponge

From the analysis, three solutions were the outcome which was the nanopsonge with polymer: crosslinker ratio 1:2 (solution A), 1:4 (solution B), and 1:8 (solution C) at a homogenization duration of 15 minutes. The outcome of the analysis was based on optimum characteristics of particle size, zeta potential, and PDI. These three solutions were then used to entrap retinoic acid and determine the nanosponge with the best entrapment efficiency.

3.2.1. Entrapment efficiency and solubilization efficiency

Entrapment of retinoic acid was done by entrapping the drug into three different nanosponges. The entrapment efficiency obtained is shown in Figure 1. An average of 75.32% (SD=0.0289), 73.69% (SD=0.0781), and 78.19% (SD=0.850) were obtained for solutions A, B, and C respectively. The different nanosponge used (1:2, 1:4, 1:8) has a significant effect (p<0.005) on the percentage of entrapment efficiency whereby there is no significant difference between solutions A and B, but there is a significant difference between solutions A & B compared to solution C (p<0.005). Hence solution C (1:8) which obtained the highest entrapment efficiency was selected for further determination of the best drug: nanosponge ratio for entrapment. A previous study that entrapped paliperidone in NS 1:4 and NS 1:8 obtained similar results whereby NS 1:8 had higher EE%[27]. Another study that entrapped calcium carbonate in B-cyclodextrin nanosponge also showed that nanosponge with polymer: crosslinker ratio of 1:8 has the highest entrapment efficiency[8]. The high entrapment efficiency obtained may be the result of higher crosslinking between BCD and CDI which permits better entrapment of retinoic acid in the nanosponge[8,27].

The polymer to crosslinker ratio shows a significant effect on the solubility efficiency (p<0.005) of the loaded nanosponge. All loaded nanosponges showed higher solubility than retinoic acid alone as presented in Figure 2 due to the structural characteristic of nanosponges.

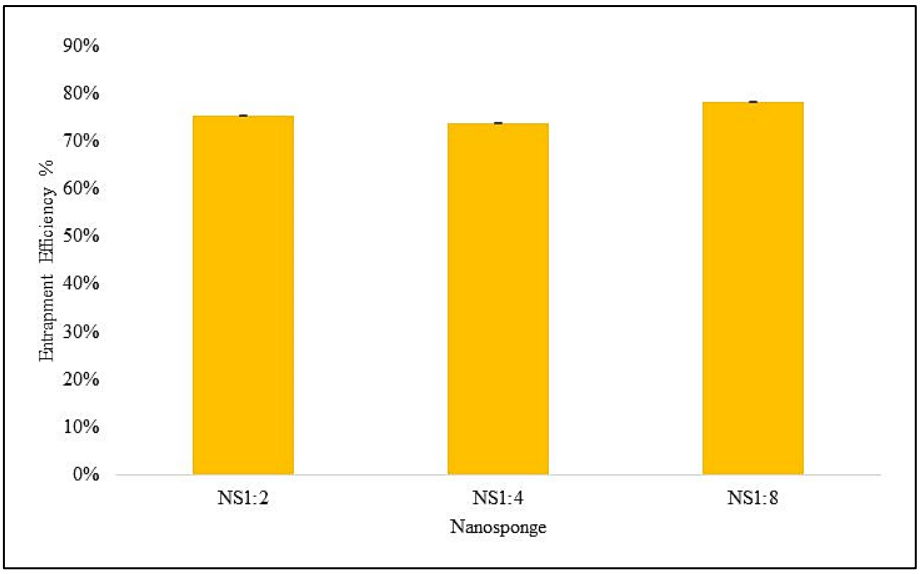

Figure 1. Entrapment efficiency nanosponge with varying polymer: crosslinker ratio.

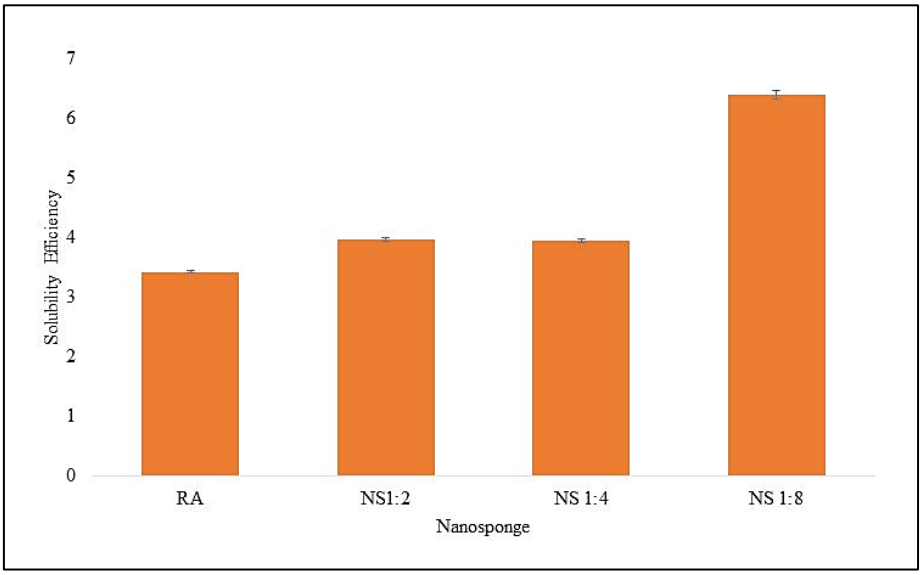

Figure 2. Solubilization efficiency of nanosponge with varying polymer:crosslinker ratio.

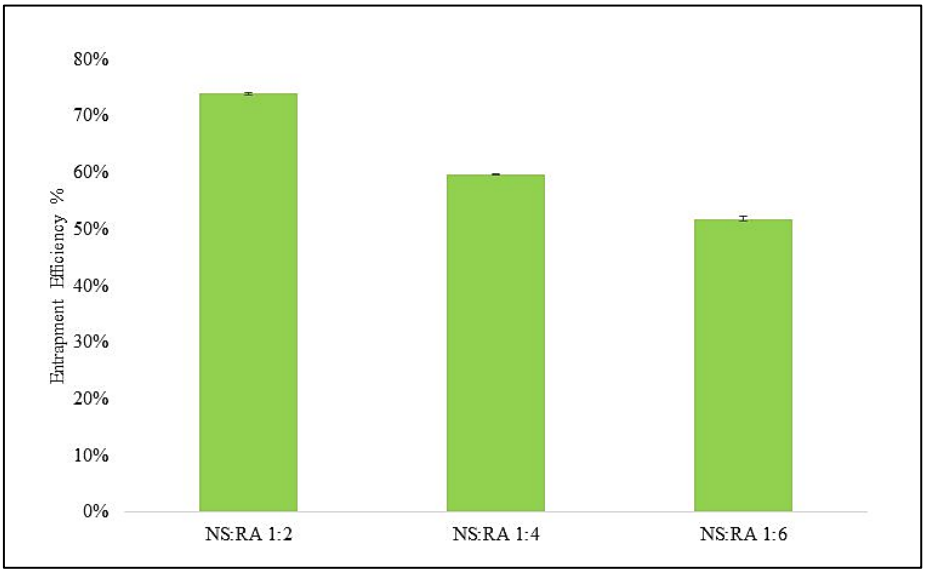

Figure 3. The entrapment efficiency of nanosponge 1:8 with varying drug:nanosponge ratio.

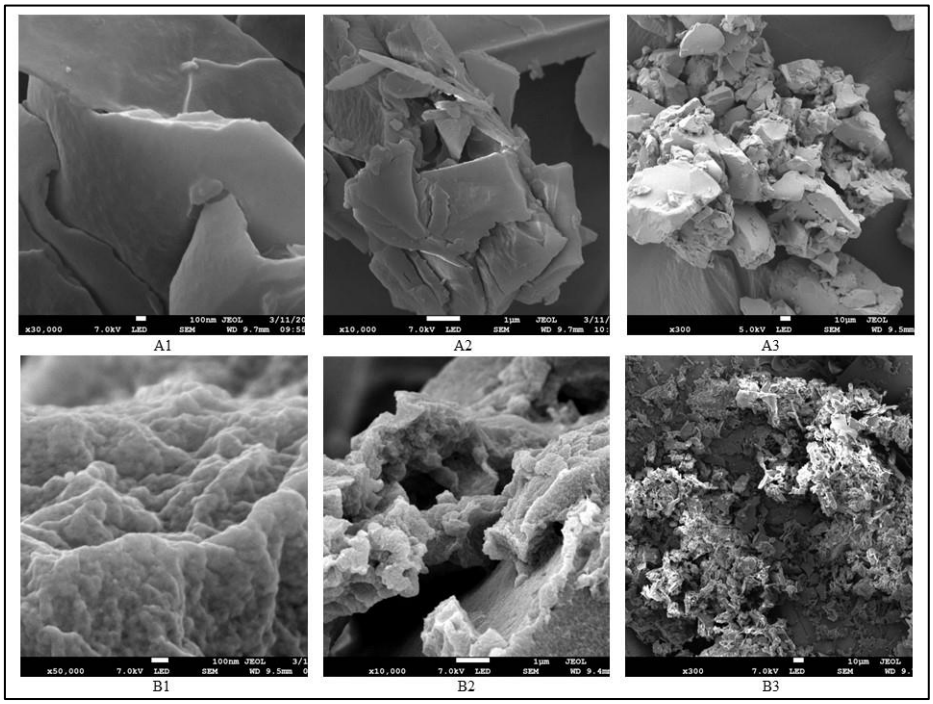

Figure 4. Field emission scanning electron microscopy of plain nanosponge at (A1) 100 nm; (A2) 1 µm (A3) 100 µm and loaded nansoponge at (B1) 100 nm; (B2) 1µm (B3) 100 µm.

Nanosponge structurally has numerous pores that may help improve the wetting property of retinoic acid and improve its solubility[27]. Ratio of BCD: CDI may be a factor affecting the solubilization capacity of retinoic acid as can be seen from the graph which shows 1:8 having significantly higher solubilization efficiency in comparison to other ratios. As the ratio increases, cross-linker concentration also increases which provides more sites for drug complexation hence improving solubilization efficiency[28].

Based on the entrapment efficiency and solubilization efficiency NS 1:8 was selected for further investigations. Three different retinoic acid: nanosponge (RA: NS) ratios of 1:2, 1:4, and 1:6 were prepared and obtain entrapment efficiency values of 73.90% (SD=0.1457), 59.73% (SD=0.0351) and 51.86% (SD=0.401) as depicted in Figure 3. One-way ANOVA analysis showed that different RA: NS ratio has a significant effect on the entrapment efficiency. This leads to a nanosponge 1:8 with the drug: nanosponge ratio of 1:2 with the highest entrapment efficiency. The graph shows a decreasing trend in EE% with RA: NS ratio 1:2 having the highest EE- well above the optimal EE% which is >60%[29]. The final nanosponge selected for further formulation was a nanosponge with polymer to crosslinker ratio of 1:8 which was prepared with retinoic acid to nanosponge ratio of 1:2 as it has high entrapment efficiency.

3.2.2. Particle size and zeta potential

The loaded nanosponge has a particle size of 193.90±2.74 nm which is desirable in topical treatment with retinoic acid as smaller particle size provides slow release and has better skin retention[7,14]. The PDI of 0.322±0.0346 is below 0.5 which indicates acceptable polydispersity[30]. The closer the PDI value to 0 indicates a monodisperse particle distribution which is favourable for better stability and drug delivery[31]. The zeta potential value was -26.17±0.513 mV which is much lower than values obtained in previous studies which ranged from -8.74 to -20.21 mV. These studies used similar nanosponge but entrapping paliperidone and resveratrol[27,32]. The zeta potential of loaded nanosponge is influenced by the different polymers, crosslinkers, and drugs being entrapped in the nanosponge. A study entrapping clobetasol propionate in nanosponge found clobetasol to have a zeta potential of 6.19 mV, yet became negative when entrapped with a value between -17.27 mV to -27.77 mV [7]. In this study, the polymer (-21.8 mV), crosslinker (-22.5 mV), and retinoic acid (-35.0 mV) are negatively charged hence causing the nanosponge to be more negative.

3.2.3. Surface morphology

FE-SEM was done to gain more insights into the shape and surface morphology of the developed nanosponge. The surface morphology is depicted in Figure 4. FE-SEM image of plain nanosponge at 1 µm and 100 nm as shown in images A1, A2, and A3 shows irregularly shaped crystals with a porous structure which is responsible to entrap retinoic acid. The retinoic acid-loaded nanosponge which is depicted in images B1, B2, and B3 shows that the porous structure visible in plain nanosponge is no longer visible. From the figure, a layer can be seen

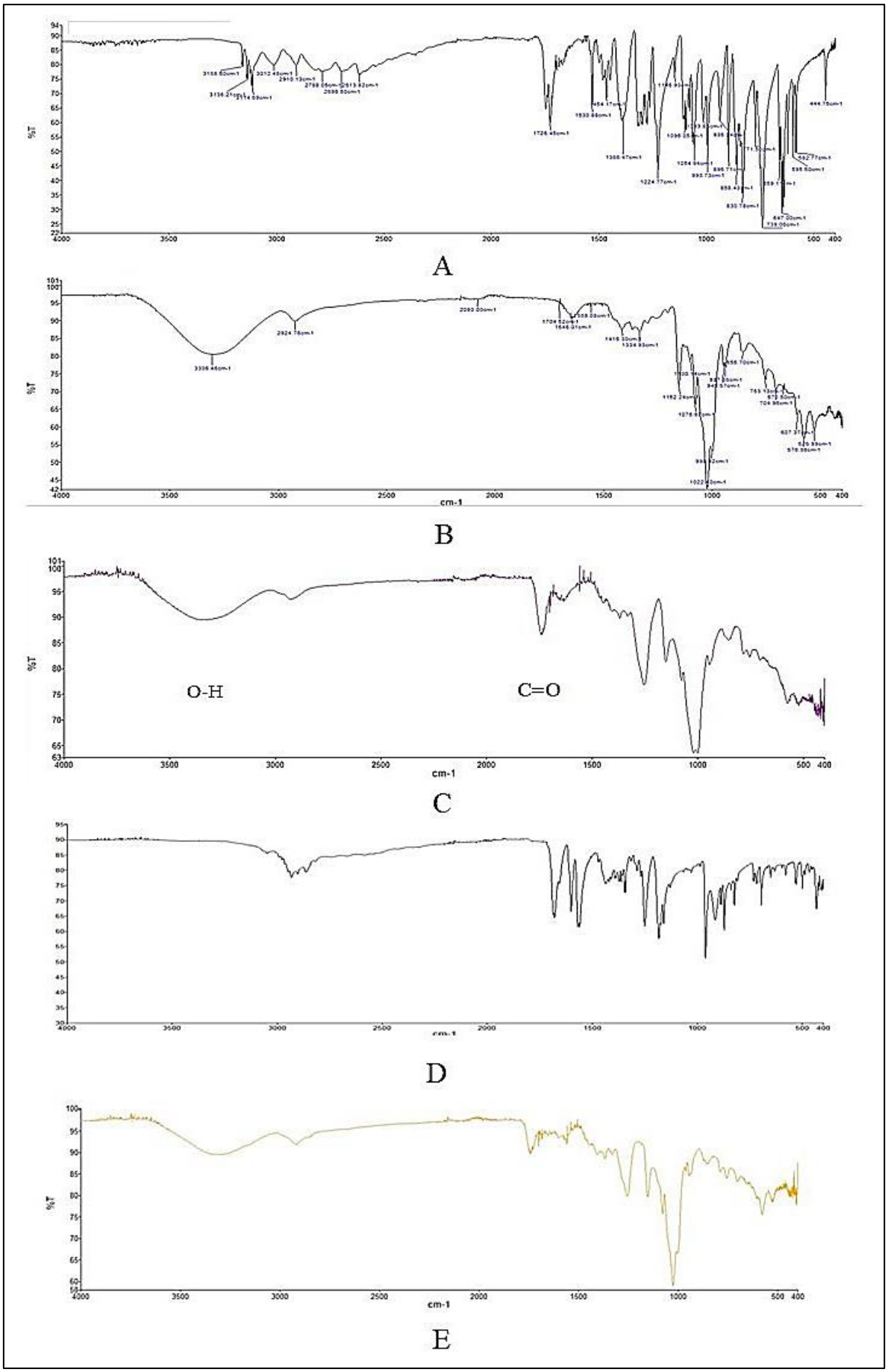

Figure 5. FTIR fingerprint of (A) carbonyldiimidazole, (B) β-cyclodextrin, (C) plain nanosponge, (D) retinoic acid, and (E) retinoic acid loaded nanosponge.

on the surface demonstrating the entrapment of retinoic acid in nanosponge which occurs through the effects of freeze drying[7].

3.2.4. ATR-FTIR Spectroscopy study

The FTIR spectrum of CDI in Figure 5 (A) shows a peak at around 1,745 cm^{-1} and 1,726 cm^{-1} due to C=O stretching as well as a peak at 1,464 cm^{-1} representing C-N stretching[33]. The FTIR spectrum of BCD in Figure 5 (B) shows characteristic peaks at 3,300-3,400 cm^{-1} due to the O-H group stretching, at 2,924 cm^{-1} due to C-H stretching, at 1,646 due to H-O-H deformation bands of water and at 1,152 cm^{-1} and 1,022 cm^{-1} indicated C-H overtone stretching[33-34]. Figure 5 (C) depicts a plain nanosponge which retains the O-H group stretch from cyclodextrin and C=O stretch from carbonyldiimidazole.

In Figure 5 (D) which is the IR spectra of retinoic acid peaks of C=O bonds of the carboxylic group are present at 1,685-1,666 cm^{-1}. The peaks attributed to the OH functional group of carboxylic acid and C-H of the double bonds are seen at 2,600-3,429 cm^{-1} [35]. The IR fingerprint of the loaded nanosponge as depicted in Figure 5 (E) confirms molecular interaction as the spectra show disappearance and shift of the retinoic acid peaks. This interaction indicates the inclusion of retinoic acid in the cyclodextrin cavity[15].

3.2.5. DSC study

The DSC thermograms of retinoic acid (blue), plain nanosponge (green), and retinoic acid-loaded nanosponge (red) are shown in Figure 6. DSC analysis of retinoic acid depicted a sharp endothermic peak at 183.5°C which indicates its melting temperature[36]. In the case of plain nanosponge, a broad peak appeared around 77.2°C corresponding to the expulsion of water content from the β-cyclodextrin cavities[28]. The DSC thermogram of retinoic acid-loaded nanosponge showed the disappearance of the melting endotherm of retinoic acid. This suggests a possible interaction of retinoic acid with nanosponge and the formation of inclusion and non-inclusion complex. After incorporation of retinoic acid in the nanosponge, the drug is entrapped and molecularly dispersed in the cyclodextrin cavity hence unable to crystallize reflecting the disappearance of its peak[15,17,36].

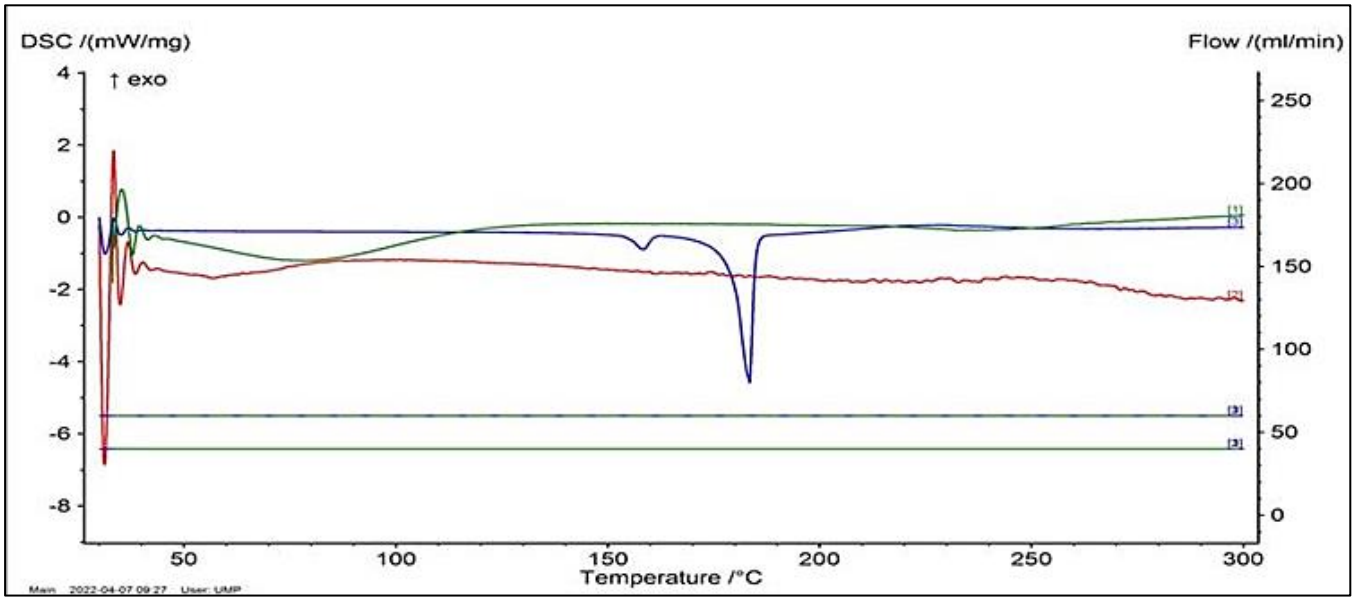

Figure 6. Overlapped Differential Scanning Calorimetry thermogram of (blue) Retinoic Acid, (green) Plain nanosponge, and (red) Retinoic acid loaded nanosponge. (Run at 40°C and 60°C is nitrogen as purge gas and protective gas, respectively).

3.2.6. In vitro Franz diffusion cells study

Figure 7 shows the cumulative amount of retinoic acid permeated from the commercial formulation while retinoic acid-loaded nanosponge gel-cream formulation on the other hand recorded a negligible amount and could not be plotted. The graph shows that the cumulative amount increased at a fast rate initially before slowing down towards the end of the study. This characteristic reflects the depletion of the drug over time which is usually seen in finite studies. The recovery of retinoic acid is presented in Figure 8. The total recovery recorded for commercial formulation is 93.03% while nanosponge formulation recorded a total of 94.17%. The recovery obtained for both formulations is in alignment with ranges suggested by both the Scientific Committee on Cosmetic Product[37] and the Organization for Economic Cooperation and Development[38] which is 85-115% and 90-110%, respectively The major percentage of recovery in commercial formulation came from the permeation (68.35%) while for nanosponge formulation the major percentage came from the skin extraction (58.73%). The

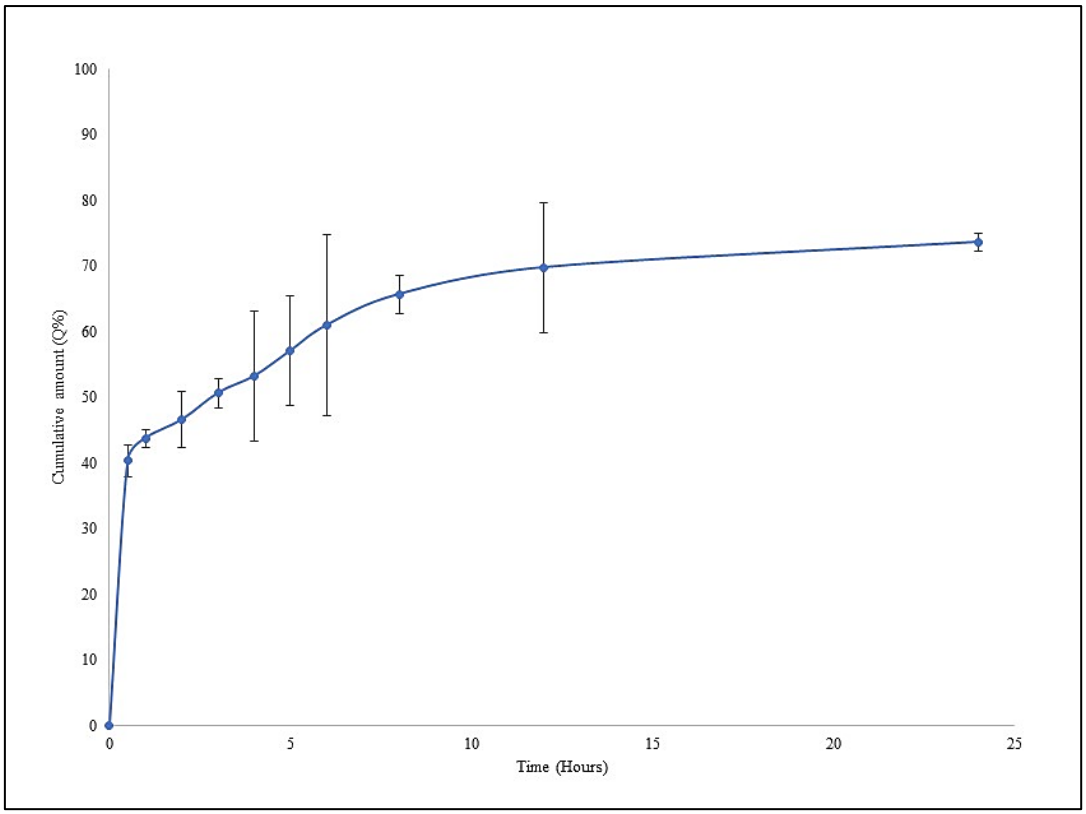

Figure 7. The cumulative amount of retinoic acid permeated through rat skin from commercial retinoic acid formulation (Mean±SD, n=8).

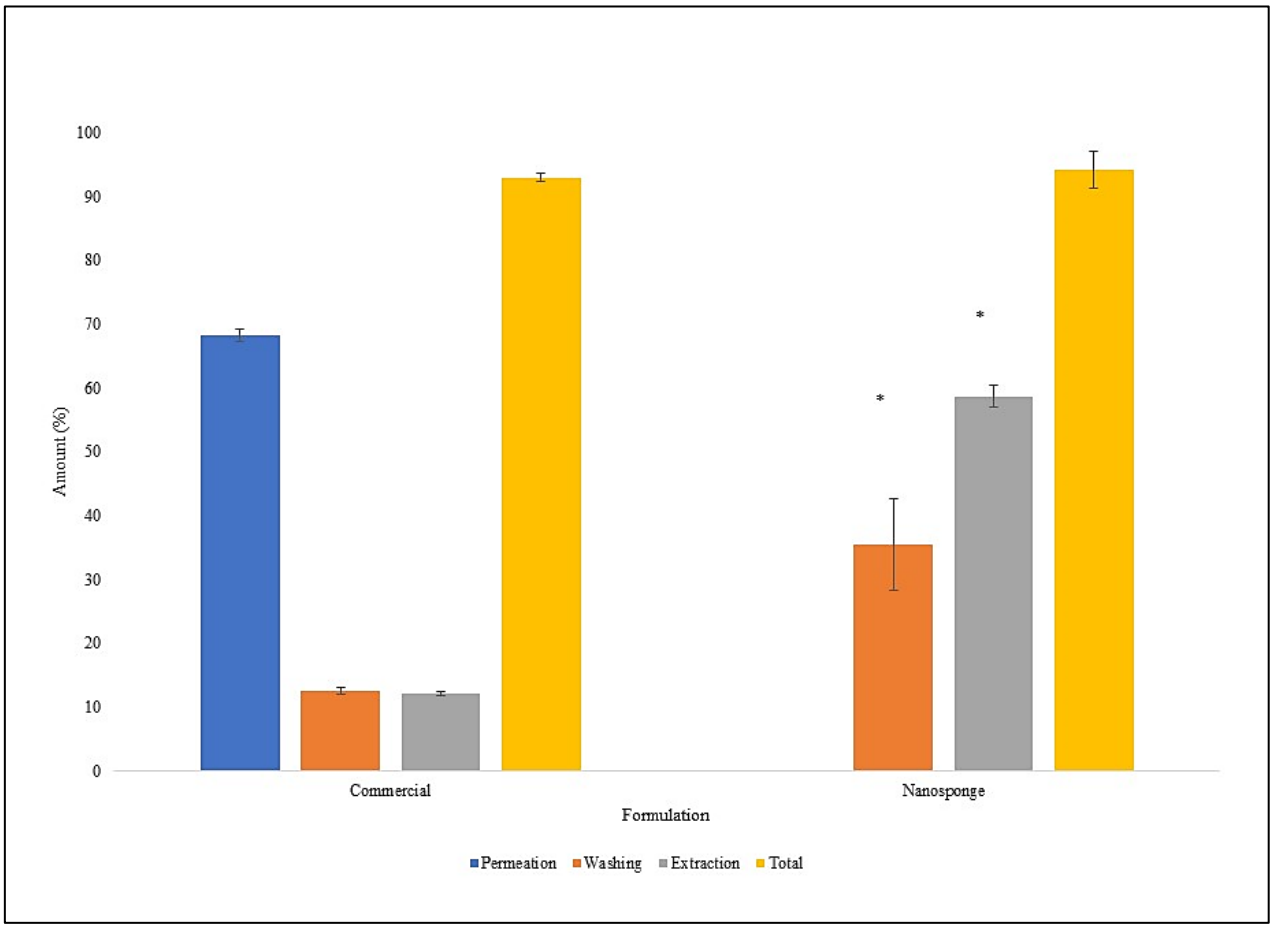

Figure 8. Total Amount of ATRA Recovered from Franz Cell Study (Mean±SD, n=8, * = p<0.05).

differences between the commercial and nanosponge groups were found to be significant (p<0.05) for permeation, washings, and extraction while the total recovery did not show any significant difference.

This indicates that nanosponge formulation mostly remained within the skin layers while commercial formulation permeated into the donor compartment which reflects permeation into blood bloodstream. The skin extraction found that 13.04% of the retinoic acid in the commercial formulation remained within the skin while 62.37% retinoic acid from the nanosponge formulation remained within the skin layers. These results show that nanosponge provides slowed and prolonged the release of retinoic acid allowing it to remain and act within the skin layers instead of penetrating the blood circulation. Prior studies also discovered findings in agreement with the current results. Encapsulation of retinoic acid in nanostructured lipid carrier (NLC) and nanocapsule did not detect or found negligible values of retinoic acid in the receptor fluid compared to its commercial counterpart[39-40]. Other studies that encapsulated retinoic acid in solid lipid nanoparticles (SLN) and NLC which did lead to permeation into the receptor fluid discovered that the release of retinoic acid became slow and prolonged[41-42]. The amount of drug released within the stipulated time was also much lower compared to the marketed formulation which released 100% of the drug by the end of the study[42]. The amount of drug extracted from the skin was also much higher in the NLC formulation compared to the commercial formulation by almost double the value[39].

5. CONCLUSION

The synthesis of cyclodextrin nanosponge and the entrapment of retinoic acid within the nanosponge produced a complex with superior characteristics. The entrapment of retinoic acid in nanosponge was proven to increase the solubilization of retinoic acid compared to the drug alone. The effect of different polymer to crosslinker ratios and speed of homogenization was studied and it was confirmed that a ratio of 1:8 and with a duration of 15 minutes has the best entrapment efficiency and increases solubilization compared to retinoic acid alone. The nanosponge was then assessed further by carrying drug: nanosponge ratio of 1:2, 1:4, and 1:6 w/w. The ratio of 1:2 showed high entrapment efficiency. The complex formation was confirmed with ATR-FTIR and DSC. The Franz diffusion cells study indicates that nanosponge maintains the action of retinoic acid within the skin layers and prevents it from absorbing into the bloodstream. Future works can further formulate nanosponge into a topical formulation for acne treatment.

6. ACKNOWLEDGEMENT

The authors acknowledge International Islamic University Malaysia (IIUM) for administrative and technical support.

Funding
There is nothing to declare.

Conflict of interest
None to declare.

Ethics approval
The study was done with an ethical approval number obtained from the Institutional Animal Care and Use Committee (I-ACUC) of the International Islamic University Malaysia (IIUM) with approval number IACUC-2020-025.

Article info:
Received August 24, 2023
Received in revised form February 4, 2024
Accepted March 15, 2024

Author contribution
Syed Omar SS collected data and wrote the paper, while Hadi HA designed the analysis and revised the paper, Doolanea Abd Almonem contributed to the analysis tool, while Zulkifli NA contributed to the data.

REFERENCES

1. Azulay DR, Vendramini DL. Retinoids. In: Daily routine in cosmetic dermatology. New York: Springer International Publishing; 2016. p. 1-16.
2. Castro GA, Oliveira CA, Mahecha GAB, Ferreira LAM. Comedolytic effect and reduced skin irritation of a new formulation of all-trans retinoic acid-loaded solid lipid nanoparticles for topical treatment of acne. Arch Dermatol Res. 2011;303(7):513-20.
3. Leyden J, Stein-Gold L, Weiss J. Why topical retinoids are mainstay of therapy for acne. Dermatol Ther (Heidelb). 2017;7(3): 293-304.
4. Leccia MT, Auffret N, Poli F, Claudel JP, Corvec S, Dreno B. Topical acne treatments in Europe and the issue of antimicrobial resistance. J Eur Acad Dermatology Venereol. 2015;29(8):1485-92.
5. Charoenputtakhun P, Opanasopit P, Rojanarata T, Ngawhirunpat T. All-trans retinoic acid-loaded lipid nanoparticles as a transdermal drug delivery carrier. Pharm Dev Technol. 2014;19(2): 164-72.
6. Torne S, Darandale S, Vavia P, Trotta F, Cavalli R. Cyclodextrin-based nanosponges: Effective nanocarrier for tamoxifen delivery. 2013;18(3):619-25.
7. Kumar S, Prasad M, Rao R. Topical delivery of clobetasol propionate loaded nanosponge hydrogel for effective treatment of psoriasis: Formulation, physicochemical characterization, antipsoriatic potential and biochemical estimation. Mater Sci Eng C. 2021;119:111605.
8. Shende P, Deshmukh K, Trotta F, Caldera F. Novel cyclodextrin nanosponges for delivery of calcium in hyperphosphatemia. Int J Pharm. 2013;456(1):95-100.
9. Kumar S, Pooja, Trotta F, Rao R. Encapsulation of Babchi oil in cyclodextrin-based nanosponges: physicochemical characterization, photodegradation, and *in vitro* cytotoxicity studies. Pharmaceutics. 2018;10(4):169.
10. Bhowmik H, Venkatesh DN, Kuila A, Kumar KH. Nanosponges: A review. Int J Appl Pharm. 2018;10(4):1-5.

11. Panda S, Vijayalakshmi S, Pattnaik S, Swain RP. Nanosponges: A novel carrier for targeted drug delivery. Int J PharmTech Res. 2015;8(7):213-24.
12. Pawar S, Shende P, Trotta F. Diversity of β-cyclodextrin-based nanosponges for transformation of actives. Int J Pharm. 2019; 565:333-50.
13. Tannous M, Caldera F, Hoti G, Dianzani U, Cavalli R, Trotta F. Drug-encapsulated cyclodextrin nanosponges. Methods Mol Biol. 2021;2207:247-83.
14. Aggarwal G, Nagpal M, Kaur G. Development and comparison of nanosponge and niosome based gel for the topical delivery of tazarotene. Pharm Nanotechnol. 2016;4(3):213-28.
15. Argenziano M, Haimhoffer A, Bastiancich C, Jicsinszky L, Caldera F, Trotta F, et al. *In vitro* enhanced skin permeation and retention of imiquimod loaded in β-cyclodextrin nanosponge hydrogel. Pharmaceutics. 2019;11(3):138.
16. Dhakar NK, Matencio A, Caldera F, Argenziano M, Cavalli R, Dianzani C, et al. Comparative evaluation of solubility, cytotoxicity and photostability studies of resveratrol and oxyresveratrol loaded nanosponges. Pharmaceutics. 2019;11(10):545.
17. Osmani RAM, Kulkarni PK, Shanmuganathan S, Hani U, Srivastava A, Prerana M, et al. A 32 full factorial design for development and characterization of a nanosponge-based intravaginal *in situ* gelling system for vulvovaginal candidiasis. RSC Adv. 2016;6(23):18737-50.
18. Aldawsari HM, Badr-Eldin SM, Labib GS, El-Kamel AH. Design and formulation of a topical hydrogel integrating lemongrass-loaded nanosponges with an enhanced antifungal effect: *In vitro*/*in vivo* evaluation. Int J Nanomedicine. 2015;10:893-902.
19. Penjuri SCB, Ravouru N, Damineni S, BNS S, Poreddy SR. Formulation and evaluation of lansoprazole loaded nanosponges. Turkish J Pharm Sci. 2016;13(3):304-10.
20. Gupta J, Mohad G, Prabakaran L, Gupta R. Emulsion solvent diffusion evaporation technique: formulation design optimization and investigation of aceclofenac loaded ethyl cellulose microspheres. Int J Drug Dev Res. 2013;5(4):336-49.
21. Srinivas P, Sreeja K. Formulation and evaluation of voriconazole loaded nanosponges for oral and topical delivery. Int J Drug Dev Res. 2013;5(1):55-69.
22. Anarjan N, Jafarizadeh-Malmiri H, Nehdi IA, Sbihi HM, Al-Resayes SI, Tan CP. Effects of homogenization process parameters on physicochemical properties of astaxanthin nanodispersions prepared using a solvent-diffusion technique. Int J Nanomedicine. 2015;10:1109-18.
23. Chaudhary V, Sharma S. Effect of various synthesis parameters on styrene–divinylbenzene copolymer properties. J Porous Mater. 2019;26(6):1559-71.
24. Nienow AW. The mixer as a reactor: Liquid/solid systems. In: Harnby N, Edwards MF, Nienow AW, editors. Mixing in the Process Industries. 2nd ed. United Kingdom: Butterworth-Heinemann; 1992. p. 394-411.
25. Wang D, Fan LS. Particle characterization and behavior relevant to fluidized bed combustion and gasification systems. In: Scala F, editor. Fluidized Bed Technologies for Near-Zero Emission Combustion and Gasification. United Kingdom: Woodhead Publishing; 2013. p. 42-76.
26. Nakatuka Y, Yoshida H, Fukui K, Matuzawa M. The effect of particle size distribution on effective zeta-potential by use of the sedimentation method. Adv Powder Technol. 2015;26(2):650-6.
27. Sherje AP, Surve A, Shende P. CDI cross-linked β-cyclodextrin nanosponges of paliperidone: Synthesis and physicochemical characterization. J Mater Sci Mater Med. 2019;30(6):74.
28. Zidan MF, Ibrahim HM, Afouna MI, Ibrahim EA. *In vitro* and *in vivo* evaluation of cyclodextrin-based nanosponges for enhancing oral bioavailability of atorvastatin calcium. Drug Dev Ind Pharm. 2018;44(8):1243-53.
29. El-Say KM. Maximizing the encapsulation efficiency and the bioavailability of controlled-release cetirizine microspheres using draper-lin small composite design. Drug Des Devel Ther. 2016; 10:825-39.
30. Torres CE, Cifuentes J, Gómez SC, Quezada V, Giraldo KA, Puentes PR, et al. Microfluidic synthesis and purification of magnetoliposomes for potential applications in the gastrointestinal delivery of difficult-to-transport drugs. Pharmaceutics. 2022;14(2):315.
31. Rosyada A, WB S, E W. Characterization of chitosan nanoparticles as an edible coating material. IOP Conf Ser Earth Environ Sci. 2019;230:012043.
32. Ansari KA, Vavia PR, Trotta F, Cavalli R. Cyclodextrin-based nanosponges for delivery of resveratrol: *in vitro* characterisation, stability, cytotoxicity and permeation study. AAPS PharmSciTech. 2011;12(1):279-86.
33. Xin WL, Lu KK, Zhu DR, Zeng HB, Zhang XL, Marks RS, et al. Highly reactive N,N′-carbonyldiimidazole-tailored bifunctional electrocatalyst for oxygen reduction and oxygen evolution. Electrochim Acta. 2019;307:375-84.
34. Rachmawati H, Edityaningrum CA, Mauludin R. Molecular inclusion complex of curcumin-β-cyclodextrin nanoparticle to enhance curcumin skin permeability from hydrophilic matrix gel. AAPS PharmSciTech. 2013;14(4):1303-12.
35. Shakiba E, Khazaei S, Hajialyani M, Astinchap B, Fattahi A. Preparation and *in vitro* characterization of retinoic acid-loaded poly(ε-caprolactone)-poly(ethylene glycol)-poly(ε-caprolactone) micelles. Res Pharm Sci. 2017;12(6):478.
36. Abdel Rahman S, Abdelmalak NS, Badawi A, Elbayoumy T, Sabry N, El Ramly A. Tretinoin-loaded liposomal formulations: From lab to comparative clinical study in acne patients. Drug Deliv. 2016;23(4):1184-93.
37. Scientific Committee on Consumer Products (SCCP). Basic criteria for the *in vitro* assessment of dermal absorption of cosmetic ingredients. SCCP/0970/06. European Commission; 2006.
38. Organization of Economic and Cooperation Development (OECD). Test No. 427: Skin absorption: *In vivo* method. OECD Guideline for the Testing of Chemicals, Section 4: Health Effects. Paris: OECD; 2004. p. 1-8.
39. Ghate VM, Kodoth AK, Raja S, Vishalakshi B, Lewis SA. Development of MART for the rapid production of nanostructured lipid carriers loaded with all-trans retinoic acid for dermal delivery. AAPS PharmSciTech. 2019;20(4):1-16.
40. Ebrahimi S, Mahjub R, Haddadi R, Vafaei SY. Design and optimization of cationic nanocapsules for topical delivery of tretinoin: application of the box-behnken design, *in vitro* evaluation, and *ex vivo* skin deposition study. Biomed Res Int. 2021; 2021:1-13.
41. Arantes VT, Faraco AAG, Ferreira FB, Oliveira CA, Martins-Santos E, Cassini-Vieira P, et al. Retinoic acid-loaded solid lipid nanoparticles surrounded by chitosan film support diabetic wound healing in *in vivo* study. Colloids Surfaces B Biointerfaces. 2020;188:110749.
42. Ghate VM, Lewis SA, Prabhu P, Dubey A, Patel N. Nanostructured lipid carriers for the topical delivery of tretinoin. Eur J Pharm Biopharm. 2016;108:253-61.